

## **CHAPTER V**

### **EXPERIMENTAL RESULTS**

#### **5.1 INTRODUCTION**

This Chapter presents the results of the investigation of accretion samples obtained from the Kalgoorlie flash smelting furnace and the laboratory using the optical microscope and SEM. The optical microscope results obtained from dust and accretions from Kalgoorlie are contained in Section 5.2 and 5.3, respectively. The SEM results obtained from accretions and dust from Kalgoorlie are contained in Section 5.4 and 5.5, respectively. The optical microscope and SEM results obtained from laboratory accretions are presented in Section 5.6 and 5.7, respectively.

#### **5.2 MICROSTRUCTURE OF ACCRETION SAMPLES FROM KALGOORLIE NICKEL FLASH SMELTER.**

##### **5.2.1. Accretion Samples from G Burner Port**

The G-3 burner port samples appear quite porous. The major

phase, dark phase, consists of a matrix which sticks together the minor phases (Figure 5.1). The samples also contain inclusions distributed throughout. The etched samples show that there are three phases appearing in the inclusion (Figure 5.2). A lamellar structure (Figure 5.3) was found intermixed with the major phases. The details of the lamellar structure will be discussed in Chapter 6. The structure of the G-4 samples (Figure 5.4) is similar to those from the G-3 samples. The major phase (light phase) of the G-4 samples look like particles which have not completely fused and are held together by a low melting point phase (dark phase, Figure 5.5).

#### 5.2.2 Accretion Samples from H-Burner Port

The unetched microstructure of an H-burner port sample is shown in Figure 5.6. The major phase (light phase) appears to be a network held together by the dark phases. The regions of major phase in these samples are larger than the major phases in G-burner port samples, and more complicated. There are dendritic structures and fine dendritic type microstructure in some regions (Figure 5.7). The lamellar structure was not found in these samples.

### 5.2.3 Accretion Samples from Appendage.

The accretions from the appendage have a porous, granular structure. The microstructure is similar to G-burner port samples. Figure 5.8 shows that the major phases (light phase) appears to form a matrix. A dendritic structure was found in some grains (Figure 5.9).

### 5.3 MICROSTRUCTURE OF THE DUST SAMPLES.

The dust particles appear to be spherical in shape (Figure 5.10). The large spherical particles contained the dendritic structure (light phase) and the dark phase which is probably a low melting point phase (Figure 5.11). The structure of the light phase is similar to the burner port samples (Figure 5.12), but it is difficult to identify this structure because the optical microscope has a low resolution and the particles are very small.

ศูนย์วิทยทรัพยากร  
จุฬาลงกรณ์มหาวิทยาลัย

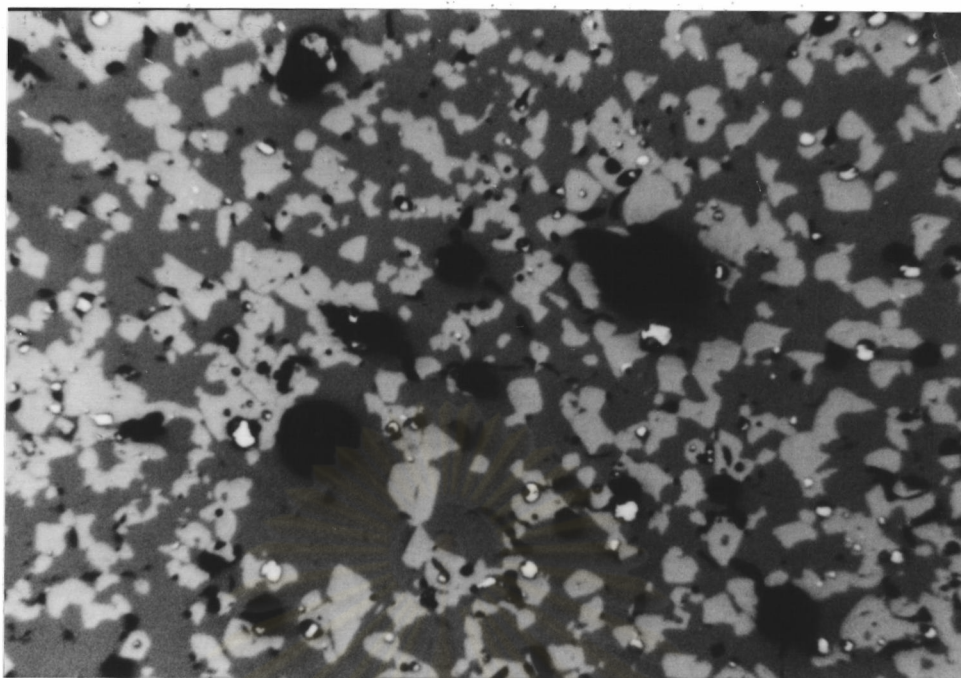


Figure 5.1 Microstructure of G-3 Sample, Etched Sample, x 50.

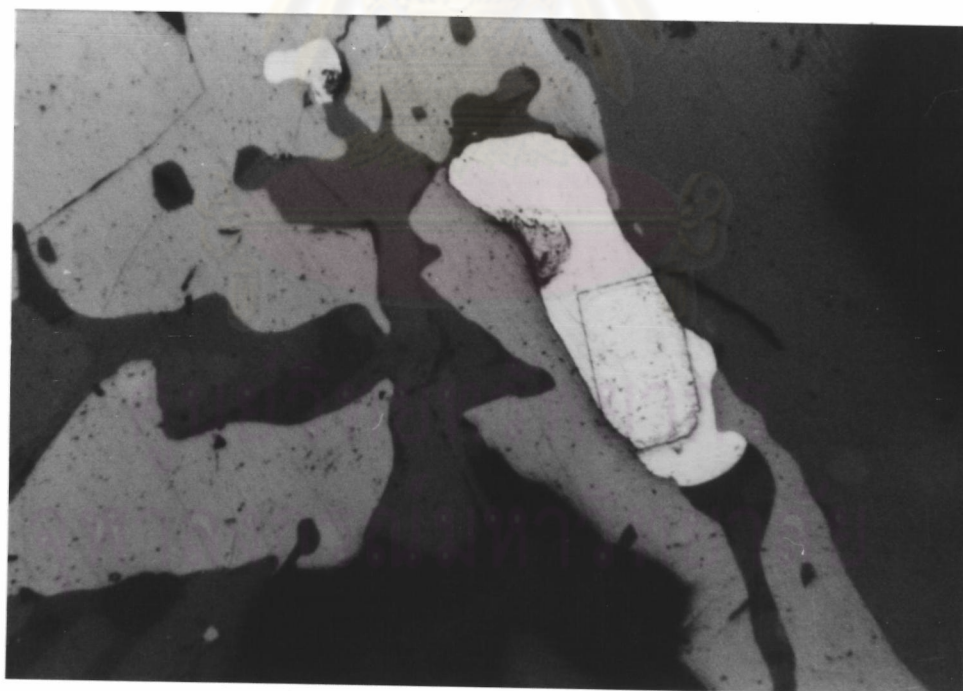


Figure 5.2 Inclusion in the G3-Burner Port Sample,  
Etched, x 200

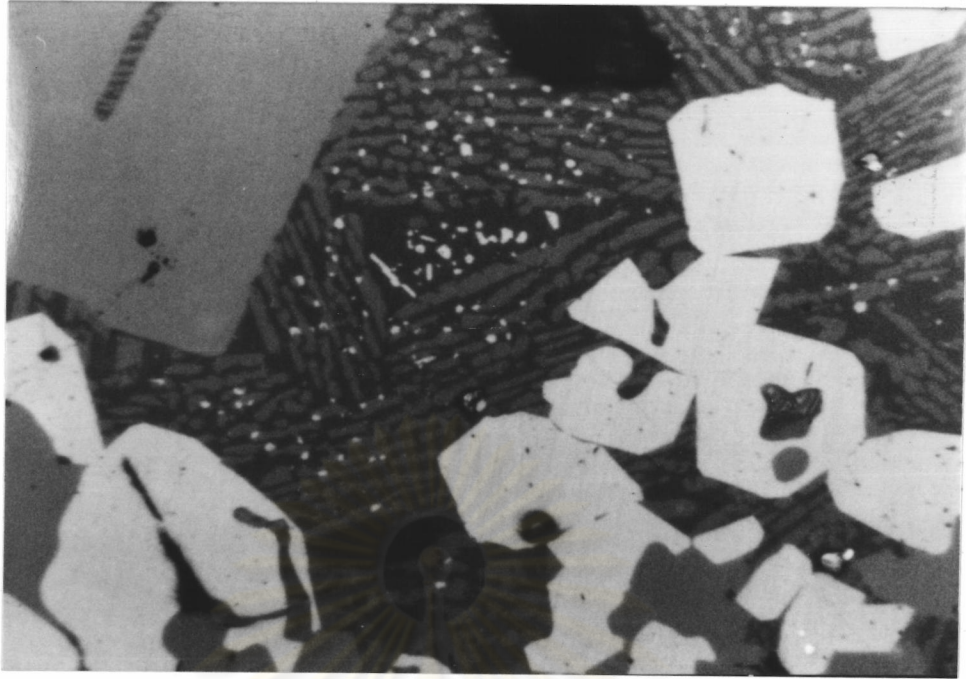


Figure 5.3 Lamellar Structure in the G-Burner Port Sample, Etched, x200.

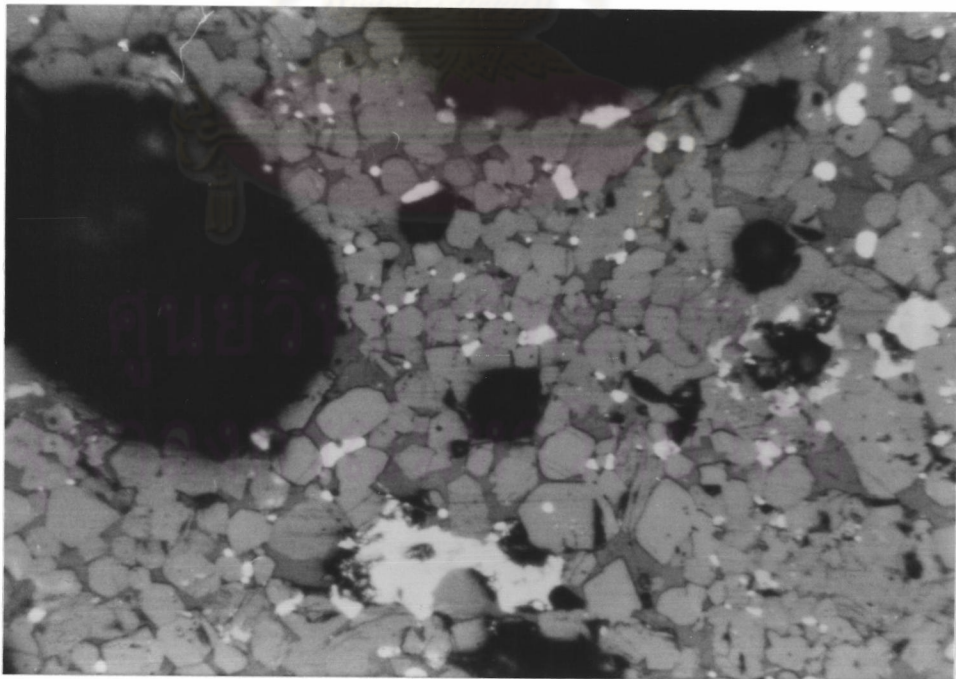


Figure 5.4 Microstructure of G-4 Sample, Unetched, x200.

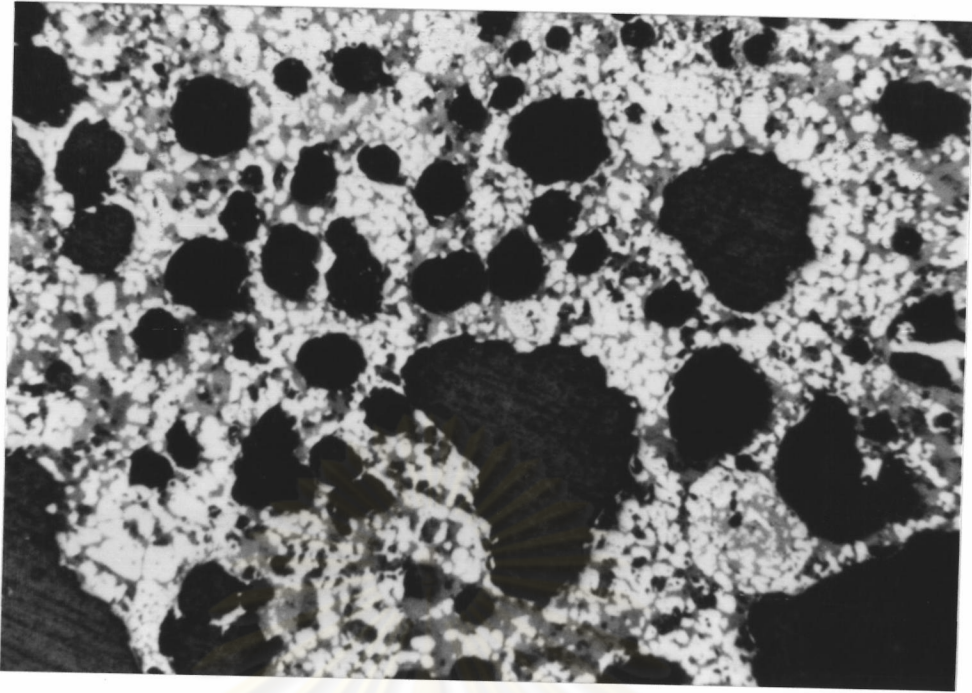


Figure 5.5 Microstructure of G-4 Samples, Unetched, x 50

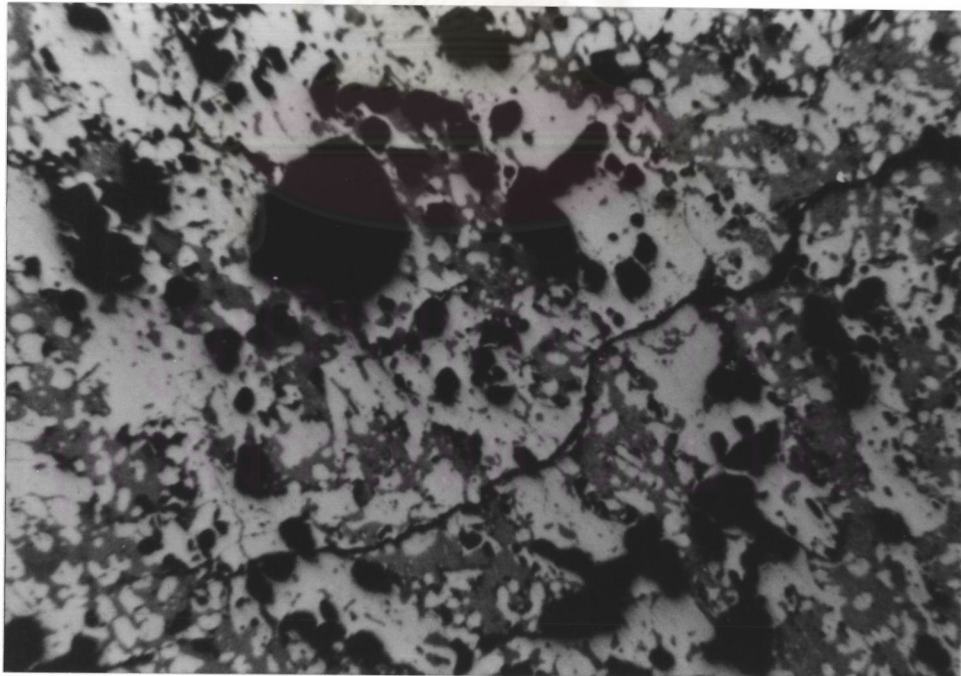


Figure 5.6 Microstructure of H-Burner Port Samples.

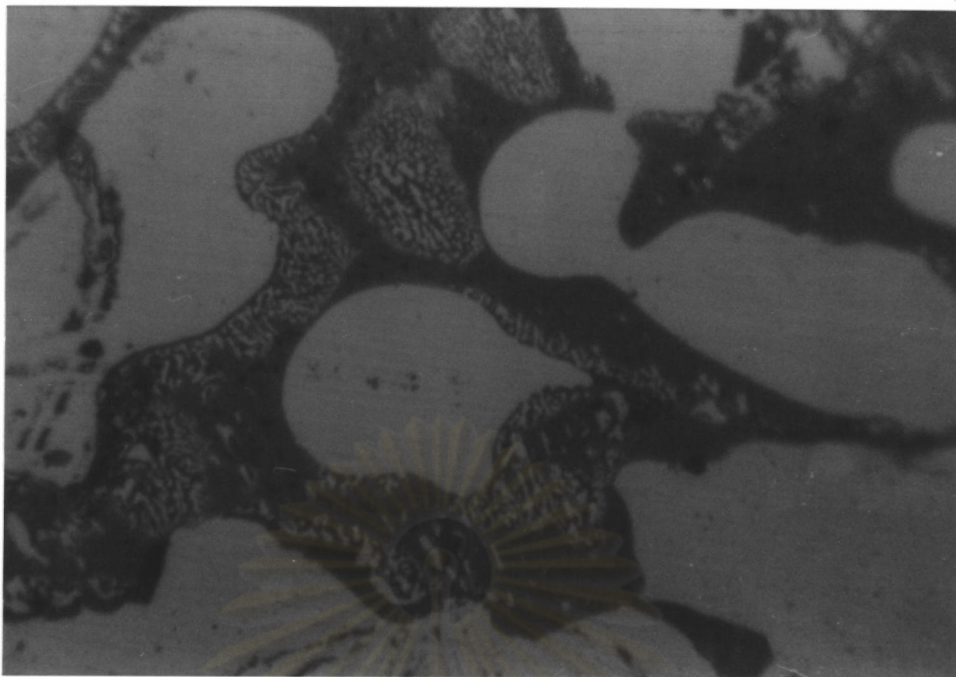


Figure 5.7 Dendritic Structure and Fine Dendritic Type Structure of H-Burner Port Sample, Etched, x 500.

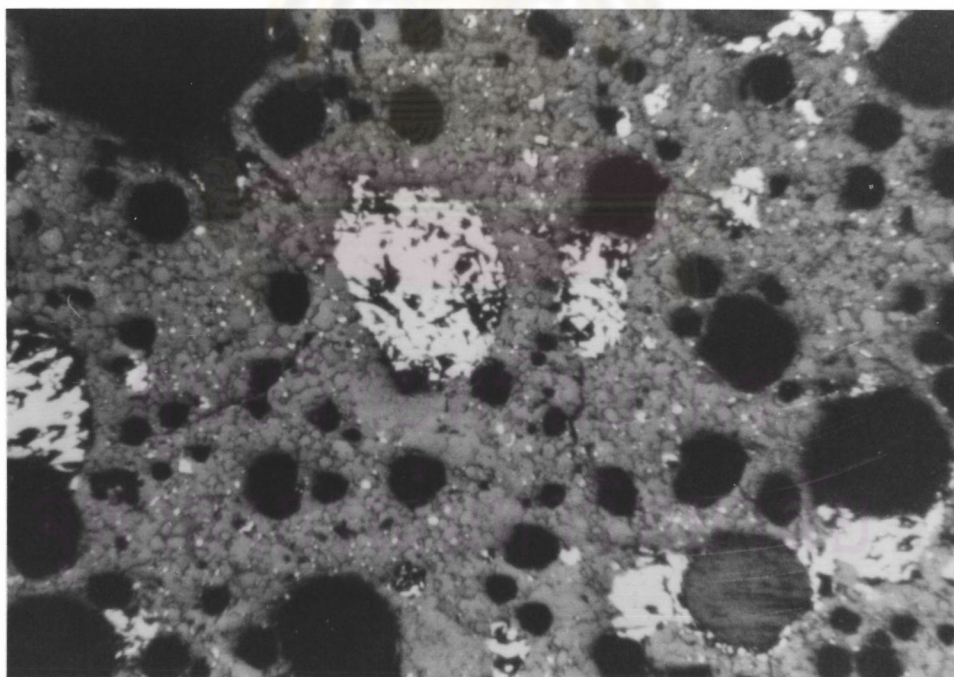


Figure 5.8 Microstructure of Appendage Sample, Unetched, x 50

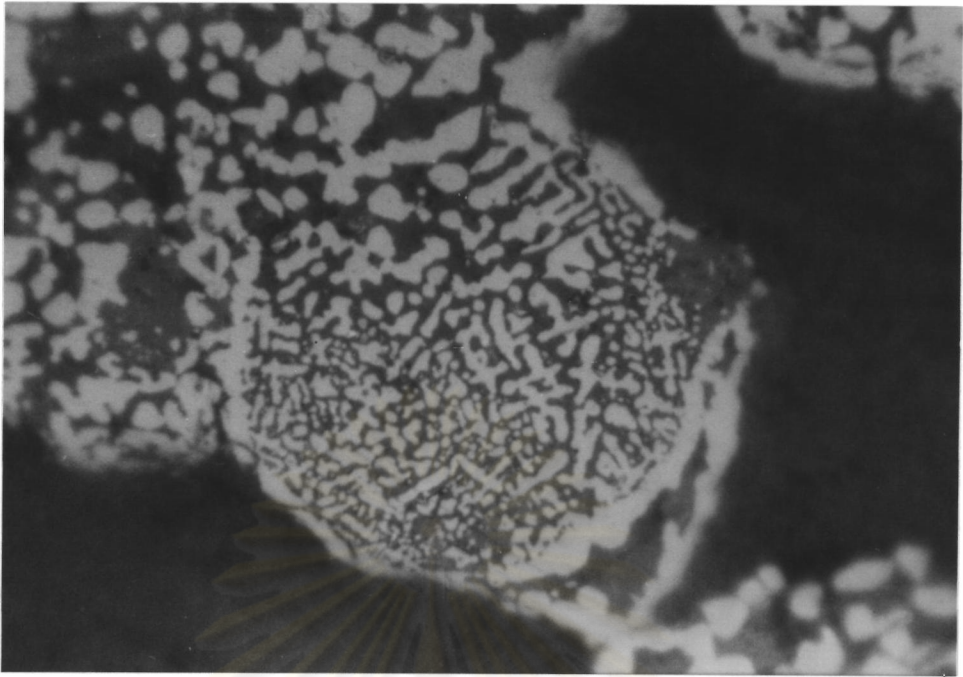


Figure 5.9 Dendritic structure was found in the appendage sample, Unetched, x 500.



Figure 5.10 Microstructure of Dust Sample, Unetched, x50.



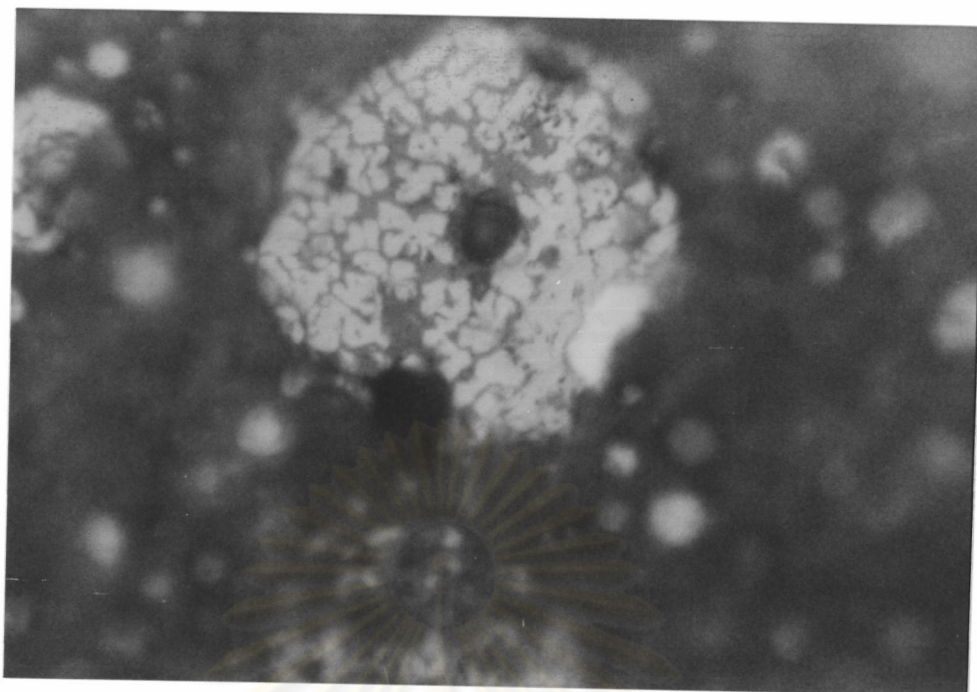


Figure 5.11 Dendritic structure in the dust sample,  
Unetched, x500.



Figure 5.12 Dendritic Intergrowths of the Light Phases of Dust  
Sample, Unetched, x500

## 5.4 SEM RESULTS FROM KALGOORLIE ACCRETION SAMPLES.

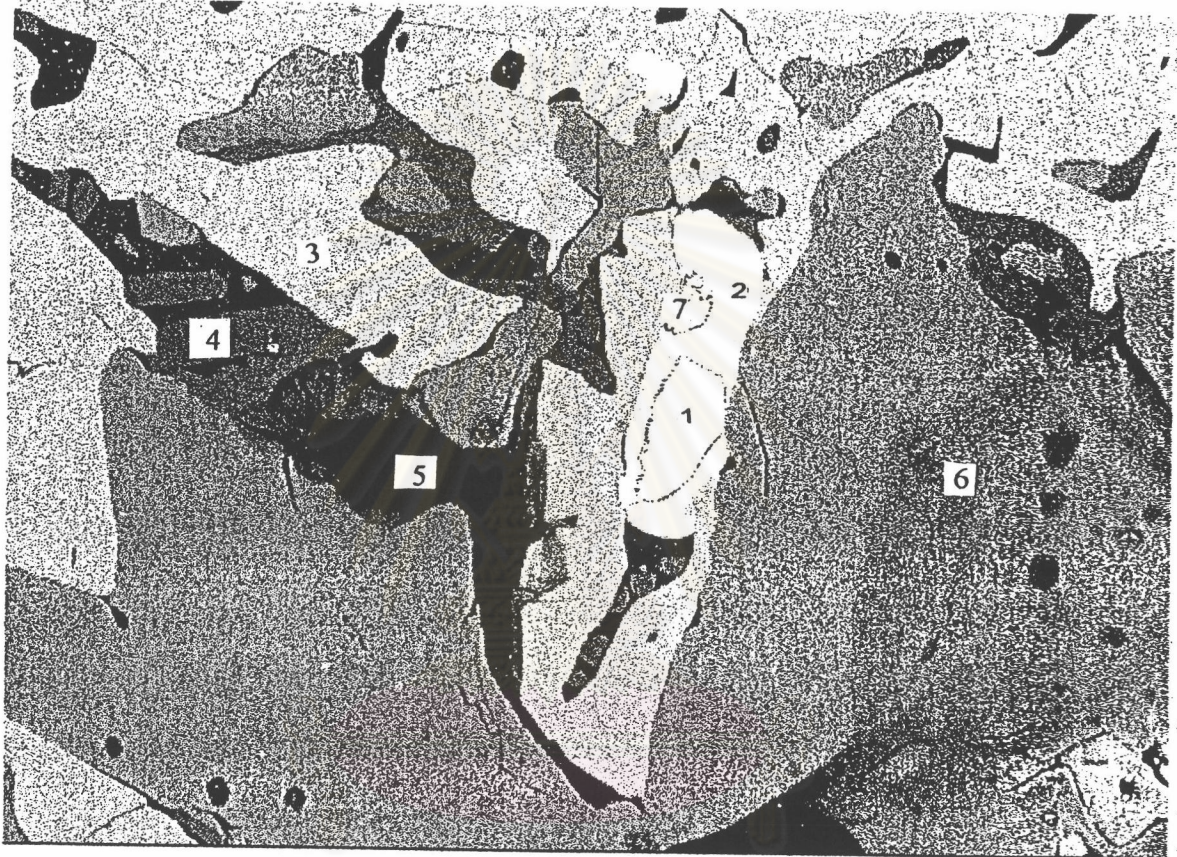
### 5.4.1 G-3 Burner Port Sample

The chemical composition of the phases in Figure 5.13 are shown on Table 5.1. The sample contained four phases and three inclusion types. The major phase (dark phase) is phase number 6, phase number 3 is the minor phase and the lamellar structure is made up of the phases number 4 and 5. Numbers 1, 2 and 7 refer to inclusions in this sample.

Table 5.1 The chemical composition of G-3 burner port sample.

No.	O	Si	Fe	Ni	Mg	Ca	Al	Cu	S
1	0.99	0.10	3.28	77.23	4.10	0.38	0.12	18.15	0.01
2	0.75	0.10	1.52	70.12	-	0.06	-	2.25	25.25
3	18.71	0.43	70.65	9.45	-	0.04	1.27	0.09	0.03
4	34.50	19.60	19.25	4.82	1.74	18.58	1.21	0.04	-
5	44.59	30.85	6.35	0.41	0.01	0.34	10.21	0.08	0.08
6	25.80	12.80	39.46	17.27	4.10	0.38	0.12	0.48	0.01
7	1.80	0.10	2.42	1.38	-	0.06	-	76.06	19.07

(w/w %)



ศูนย์วิทยทรัพยากร  
จุฬาลงกรณ์มหาวิทยาลัย

Figure 5.13 Microstructure of G-3 Burner Port Sample,  
SEM, x1500

#### 5.4.2 Chemical Composition and Microstructure of the Lamellar Structure in H4 Samples.

The lamellar structure in the H-burner port sample has been investigated by SEM. The chemical compositions are shown in Table 5.2. The light band has a high aluminium content, while the dark band has a high calcium content.

Table 5.2 Chemical composition of the lamellar structure

	O	Si	Fe	Ni	Mg	Ca	Al	Cu	S
Dark	28.45	20.97	28.41	0.77	0.10	18.57	1.39	0.00	0.04
Light	46.07	35.60	3.35	0.13	2.01	1.16	8.83	0.00	0.07

(w/w %)

#### 5.4.3 Chemical Composition of the H-Burner Port Accretion.

The chemical composition of the phases in Figure 5.7 are shown in Table 5.3. The major phase (light phase) contains high nickel and magnesium. The minor phase contains iron and nickel oxides. The dendritic phase shows composition similar to the major phase, but contained high iron and silica content.

Table 5.3 Chemical Composition of H-Burner Port Sample

	O	Si	Fe	Ni	Mg	Ca	Al	Cu	S
Major	31.3	15.2	20.3	18.9	6.8	-	-	-	-
Minor	15.8	0.4	69.6	14.5	0.8	-	0.3	-	-
Dendritic	27.4	40.6	38.4	7.9	0.9	0.4	2.4	-	-

(w/w %)

Table 5.4 Chemical Composition of the Dust Particle in Figure 5.11

	O	Si	Fe	Ni	Mg	Ca	Al	S
light	26.71	2.39	65.15	1.91	1.58	-	0.73	1.53
dark	30.84	12.96	50.81	0.53	3.57	1.08	0.04	0.17

(w/w %)

ศูนย์วิทยทรัพยากร  
จุฬาลงกรณ์มหาวิทยาลัย

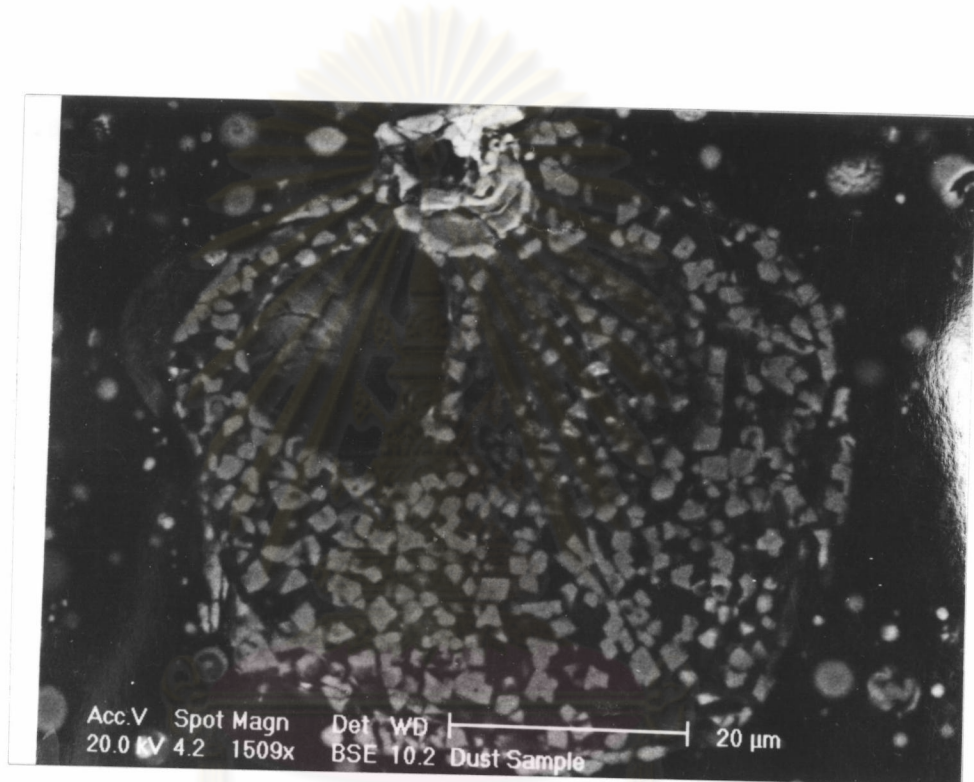
### 5.5 CHEMICAL COMPOSITION OF THE DUST SAMPLES.

The chemical composition of the dust structures in Figure 5.11 are shown in Table 5.4. The flash furnace dust, Figure 5.14, contained particles of light phase (structure number 1) and dark phase (structure number 2). The chemical composition of the structures in Figure 5.14 are shown in Table 5.5.

Table 5.5 Chemical Composition of the Structures in Figure 5.14

No.	O	Si	Fe	Ni	Mg	Ca	Al	Cu	S
1	29.88	4.97	52.95	4.25	6.07	0.30	1.76	-	-
2	45.52	18.92	20.73	0.58	12.16	0.36	1.87	-	-
3	26.19	0.63	7.45	64.06	1.02	-	0.51	-	0.21
4	2.66	0.35	5.49	77.29	0.59	0.30	0.31	-	13.00

(w/w %)



ศูนย์วิทยทรัพยากร  
จุฬาลงกรณ์มหาวิทยาลัย

Figure 5.14 Microstructure of Dust Particles, Unetched, x200

## 5.6 THE OPTICAL MICROSTRUCTURE OF LABORATORY ACCRETIONS.

The microstructure of laboratory accretions created at a constant oxygen potential equal to  $-40$  Kcal and temperature of  $1350^{\circ}$  C are shown in Figure 5.15 and 5.16. The samples contained small grains of light phases distributed throughout, while the dark phases are the minor phases. There is a structure which looks like a eutectoid structure (details shown in Chapter 6) in the dark phases, Figure 5.15. Figure 5.16 shows the columnar structure (details shown in Chapter 6) at the edges of the pores, and a dendritic structure around the pores. The 1353-55 samples contained the matrix of light phases (Figure 5.17), the dendritic structure around the pores (Figure 5.18) and some eutectoid structure in the dark phases. The microstructure of the 1353-60 sample is shown in Figure 5.19. The sample consisted of the matrix of the light phase, the eutectoid structure, and the dark phase (minor phase). Figure 5.20 shows that the microstructure of the 1403-40 sample contained the matrix of light phases, a dendritic structure in the light phase which is similar to the dendritic structure in dust samples in some regions, a eutectoid structure, and a fine dendritic structure which has a chemical composition similar to a eutectoid structure (see Chapter 6).



It was found that the amount of the eutectoid structure decreased with increasing oxygen potential. The 1403x-50 sample consisted of a fine structure (average grain size  $< 200 \mu\text{m}$ ) of the light phase (Figure 5.21) with spherical shaped pores and some cracks.



ศูนย์วิทยทรัพยากร  
จุฬาลงกรณ์มหาวิทยาลัย

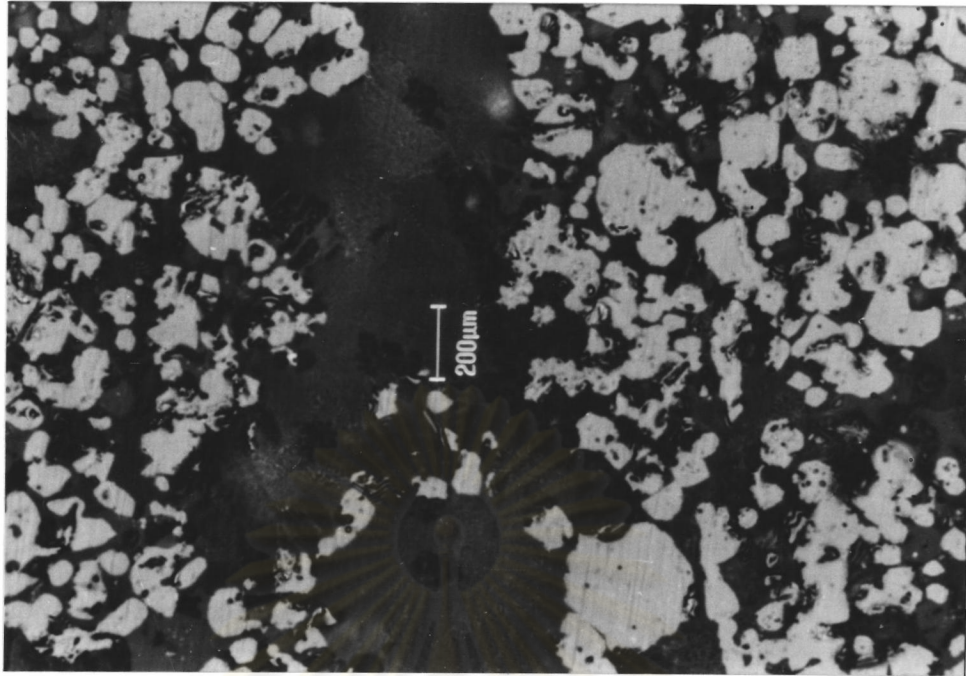


Figure 5.15 Microstructure of 1353x-40 Sample, Etched, x500.



Figure 5.16 Columnar Structure and Dendritic Structure around the Pores in 1353x-40 Samples, Etched, x500.

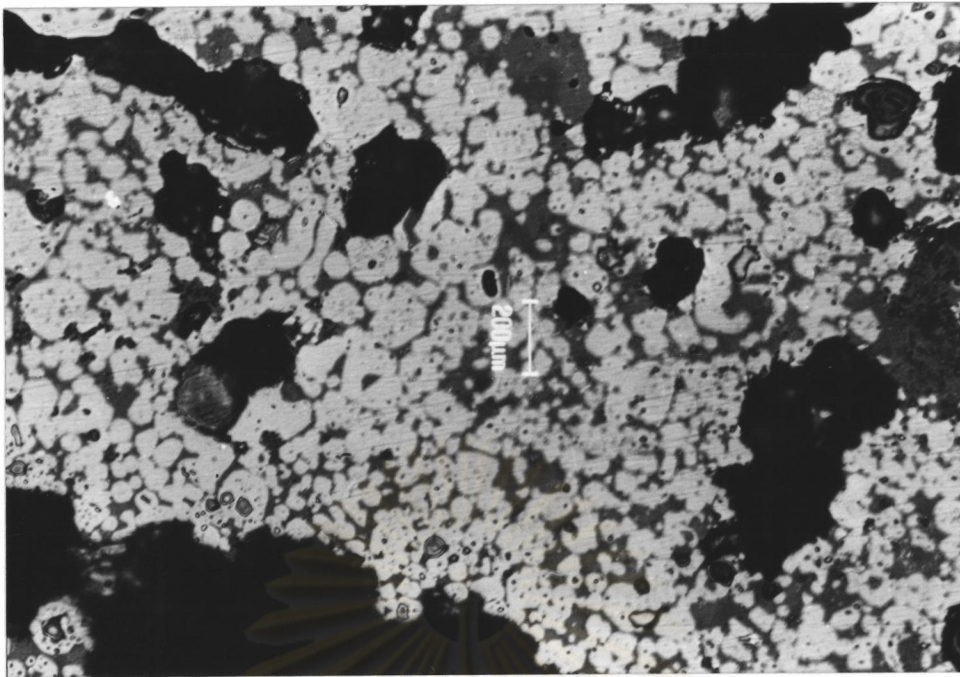


Figure 5.17 Matrix of the Light Phases in the 1353x-55 Sample, Etched, x500.

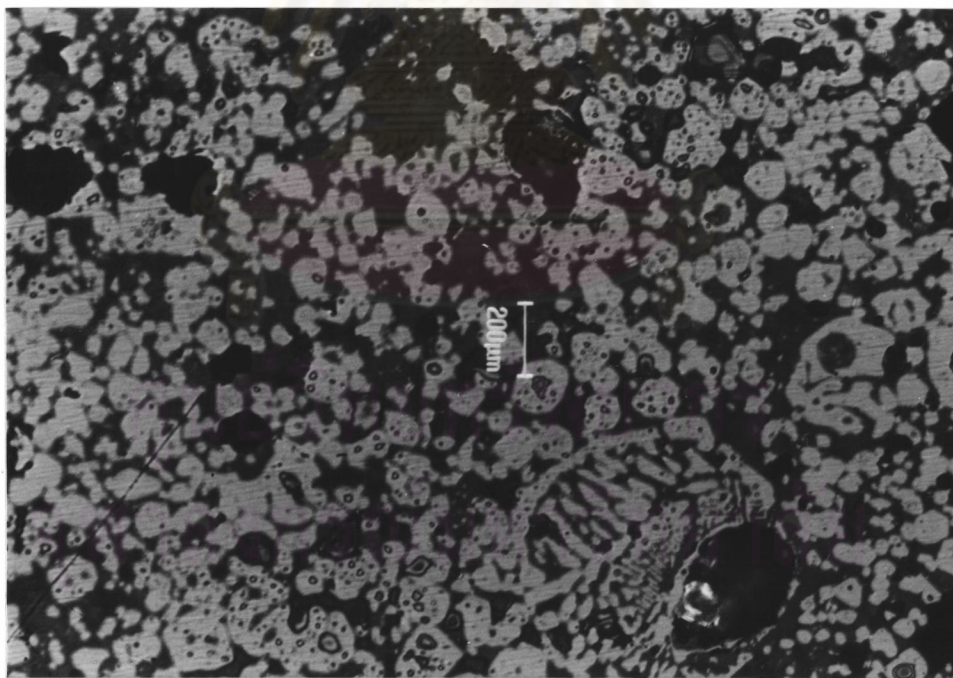


Figure 5.18 Dendritic Structure around the Pores in the 1353x-55 Samples, Etched, x500.

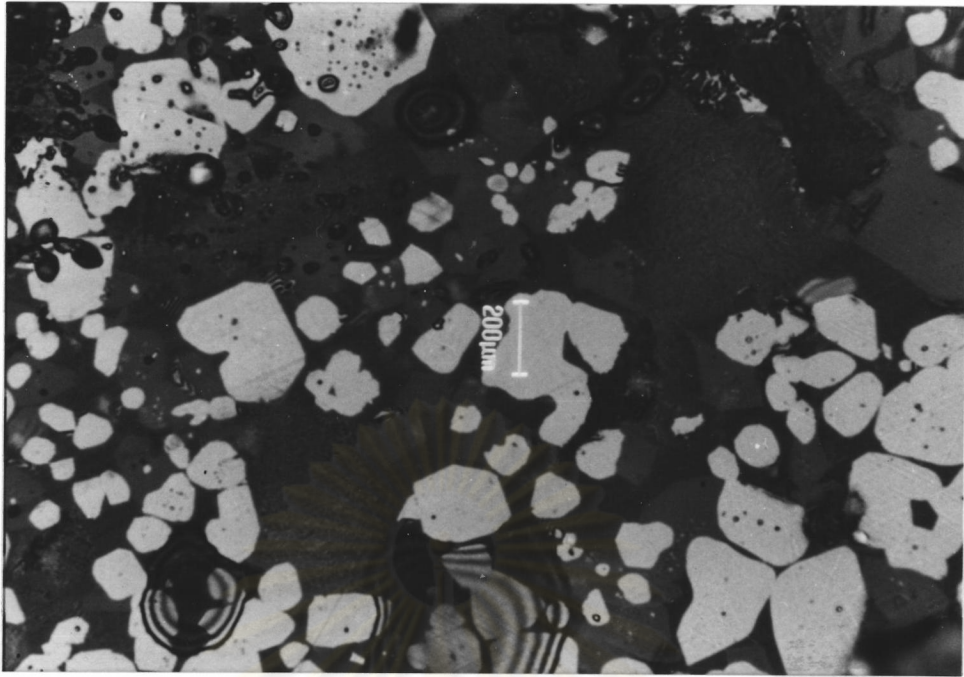


Figure 5.19 Microstructure of 1353x-60 Sample,  
Etched, x1000

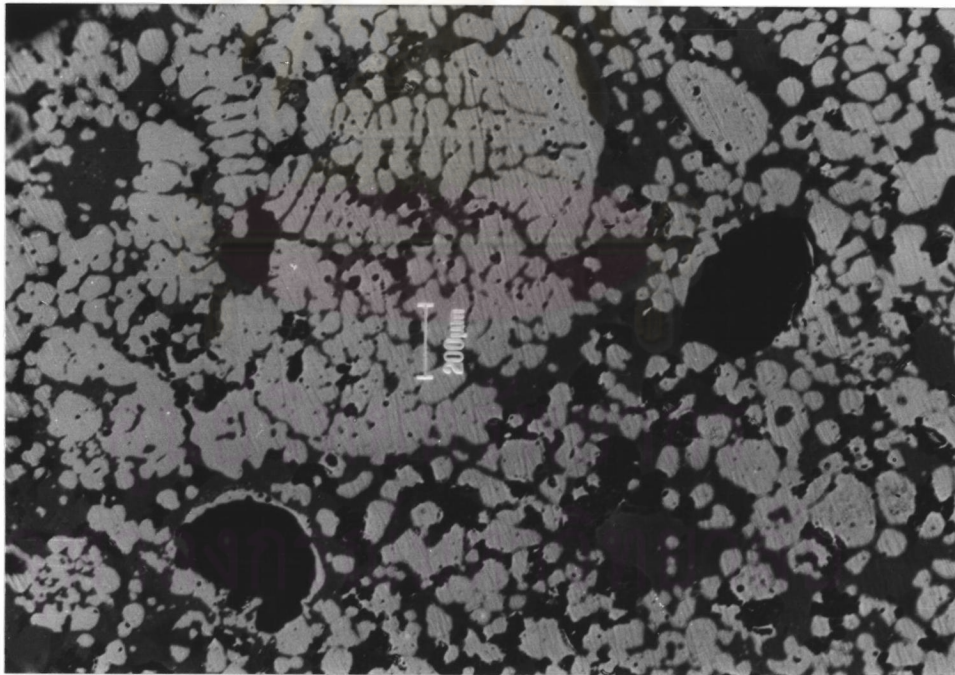


Figure 5.20 Matrix of Major Phases and the Dendritic Structure  
around the Pores in the 1403x-40 Sample,  
Etched, x500.

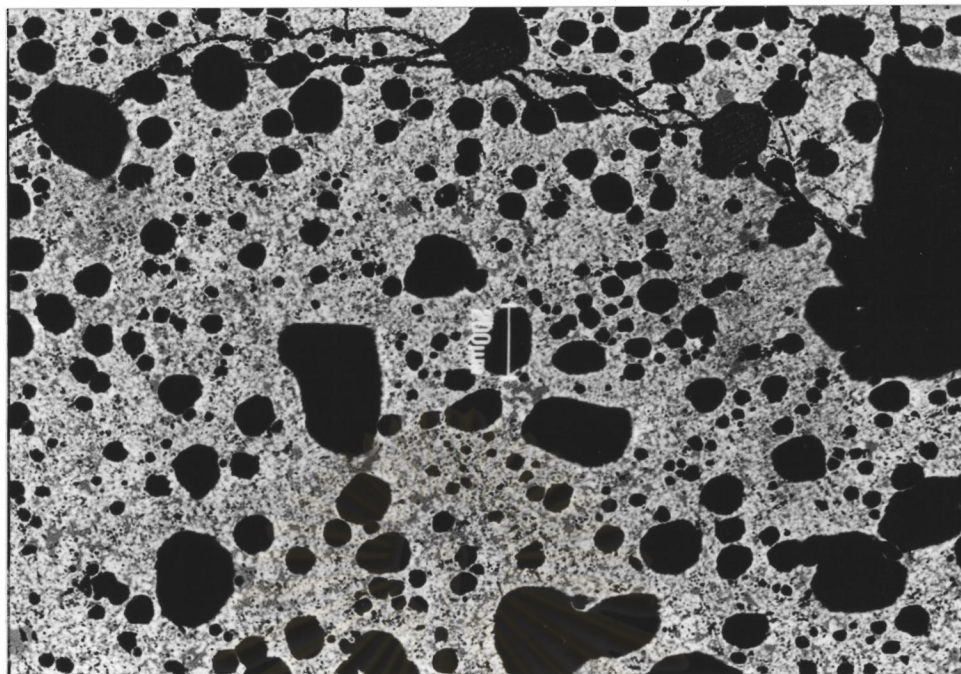


Figure 5.21 Microstructure of 1403x-50 sample contained a lot of spherical pores, x50.

Table 5.6 Chemical Composition of 1353-40 Sample

Structure	O	Fe	Si	Mg	Ca	Ni	Cu	Al
Light phase	28.70	47.71	0.88	3.11	-	17.44	0.88	1.29
Dark phase	33.86	5.59	16.68	19.11	-	24.39	0.47	-
Eutectoid Structure	43.75	4.92	31.28	2.46	7.21	0.43	1.43	3.62

(w/w %)

The microstructure of the samples produced at low oxygen potential exhibited a finer structure than the samples produced at higher oxygen potential. It was found that there are a lot of dendrites of the light phase around the pores. A structure similar to martensite was observed in the samples which were produced at 1400° C and, for the samples produced at 1350 °C, this structure was found in the 1353x-40 samples only. The structure which looked like a eutectoid structure was found in some samples.

#### **5.7 THE INVESTIGATION OF LABORATORY ACCRETIONS USING SEM.**

The major phases (light phases) of all samples contained high iron and nickel oxides. The minor phases contained high silica, high nickel and high magnesium oxides. It was found that the eutectoid structure is made up of dendrites of silica and calcium oxides with a low magnesium and aluminium oxide content. The chemical composition of the 1353x-40, 1403x-40 are shown in Tables 5.6 and 5.7.

Table 5.7 Chemical Composition of 1403-40 Samples.

Structure	O	Fe	Si	Mg	Ca	Ni	Cu	Al
Light Phase	20.15	55.73	0.26	1.82	-	20.61	0.57	0.86
Dark Phase	36.27	3.97	24.68	15.97	-	17.56	0.47	1.08
Dendritic Structure	26.31	52.61	1.28	1.42	-	16.76	1.02	0.60
Eutectoid	46.71	4.92	31.28	1.67	6.84	0.71	2.02	4.60

(w/w %)

ศูนย์วิทยทรัพยากร  
จุฬาลงกรณ์มหาวิทยาลัย